In-vacuum undulators

The in-vacuum undulator is an insertion device (ID) adopted as a standard light source at SPring-8. Because magnet arrays are contained in the vacuum chamber, the magnetic field of the in-vacuum undulator is much stronger than that of conventional undulators. In order to construct in-vacuum undulators, many techniques and procedures have been developed: magnetic-field correction, attachments for impedance reduction and bake-out systems for ultra-high vacuum. The first four devices were installed in the SPring-8 storage ring from November 1996 to February 1997, and the first radiation was observed in April 1997 without any problem.

Introduction

The insertion device is one of the most important apparatus determining the performance of a synchrotron radiation facility. In order to meet the various requirements of users, many kinds of insertion devices (IDs) such as elliptic wiggler, in-vacuum, helical and figure-8 undulators have been constructed and installed in SPring-8 [1-5]. Using these IDs makes it possible to obtain photons with circular and linear polarization in the energy range between 100 eV and 300 keV. Among them, the in-vacuum undulator is regarded as a standard ID at SPring-8. It provides an X-ray between 5 keV and 80 keV using up to the 5th harmonic.

The in-vacuum undulator is an ID with magnet arrays inside the vacuum chamber. Because no obstacle exists within the magnet gap (*i.e.*, no intervening vacuum-chamber wall), the vacuum gap is equal to the magnet gap, meaning that the vertical aperture is variable. Thus, the in-vacuum undulator is suitable for the commissioning of the storage ring. Therefore, four in-vacuum undulators were installed before starting commissioning of the storage ring. The in-vacuum undulators have another advantage in that the magnetic field is stronger than that of the conventional IDs of out-of-vacuum type. In order to construct in-vacuum undulators, many techniques have been developed at SPring-8. This report provides an outline of these techniques.

Figure 1: Photograph of in-vacuum undulator; ion and NEG pumps are not attached yet.

Specifications

Figure 1 is a photograph of the in-vacuum undulator. The specifications of the device are shown in Table I. Each 4.5 m undulator consists of three1.5 m segments. The mechanics, vacuum chambers and pumps are all standardized for easy maintenance and mass production. The periodic length of 32 mm was determined so that the energy of the 1st harmonic could range from 5 keV to 18 keV. Actually, up to 80 keV is possible by using 3rd and 5th harmonics. Figure 2 is a photograph of one magnet unit used in the in-vacuum undulator. In order to achieve an ultra-high vacuum, mechanical clamps are used to fix the magnet block instead of glue.

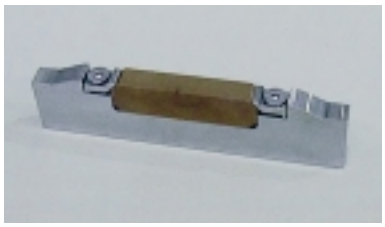

Figure 2: One magnet unit of the in-vacuum undulator; four magnet units form one period.

Table I *: Specifications of the standard in-vacuum undulator at SPring-8.*

Type	Pure Permanent Magnet
Magnet material	NdFeB
Length	4.5 m
Periodic length	32 mm
Number of periods	140
Minimum gap	8 mm
Maximum K value	2.3
Available energy (1st harmonic)	5 keV ~ 18 keV

Field Correction

Because the magnets forming the ID field are not perfect, some corrections are necessary before installation. In general, there are two kinds of field corrections. One is spectral correction for restoring spectral intensity of radiation, and the other is multipole correction for reducing the multipole component of the ID field error. In both cases, chip magnets are inserted into holes made in magnet holders to increase or reduce the magnetic field. Chipping is used instead of shimming for field correction to avoid an increase in impedance.

For spectral correction, the conventional method is to reduce the optical phase error [6]. At SPring-8, however, another quantity called error storage is used to estimate the spectral performance [7]. This represents how the field error is stored at each period of the ID and is closely related to the optical phase error. Because the error storage is found by a simpler calculation than that for optical phase, the procedure for spectral correction is simplified. For the multipole correction, special holders in which more chip-magnets can be inserted are attached to both ends of the magnet arrays, and a chip-magnet arrangement is determined to minimize the multipole component by the simulated-annealing method [8]. In the calculation, the dipole components are neglected because steering coils located upstream and downstream can easily correct them.

Figure 3 shows an example result this spectral correction. The peak flux density at each harmonic normalized by the ideal value is shown before and after spectral correction. The standard deviations of the error storage before and after correction are 5.5% and 1.3%, respectively. With an increase in harmonic number, the restoration of intensity is more remarkable. For example, the normalized flux density at the 11th harmonic before correction is only 23% of the ideal one, while that after correction is 60%. It should be noted that the standard deviations of the peak field at each magnet pole before and after correction are 0.34% and 0.32%, respectively, meaning that the restoration of intensity is not a result of a reduction in the deviation of the peak field. In addition, the r.m.s. phase error before and after spectral corrections are 15.4 and 3.9 degree, respectively, showing that the reduction in error storage causes the reduction in phase error. From these observations, we can conclude that reducing error storage is an adequate method of spectral correction.

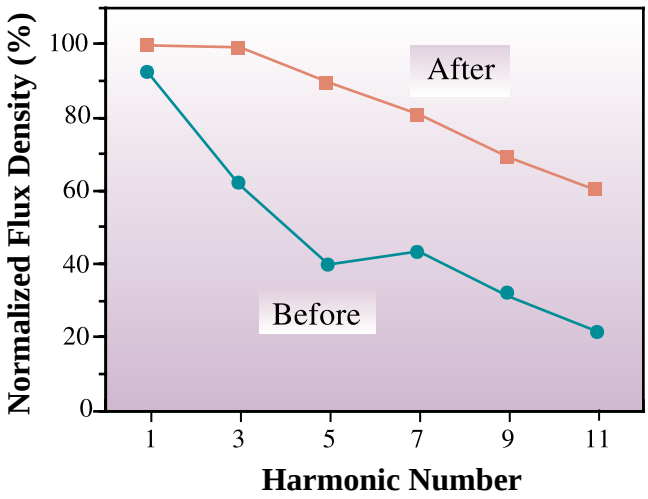

Figure 3: Comparison of the normalized flux density for various harmonics before and after spectral correction.

Table II shows an example result of multipole correction. Normal-quadrupole, normal-sextupole, skew-quadrupole and skew-sextupole components are shown as functions of the gap before and after multipole correction. Clearly, all multipole components were reduced considerably.

Table II : Multipole components before and after correction.

Gap (mm)	Normal Quad. (G.cm/cm)		Normal Sext. (G.cm/cm^2)		Skew Quad. (G.cm/cm)		Skew Sext. (G.cm/cm^2)	
	Beafre	After	Beafre	After	Beafre	After	Beafre	After
8	343	4	-97	25	-11	-11	-207	2
10	306	23	-80	-1	11	-5	-148	23
12	275	29	-69	-42	27	-4	-102	11
15	238	26	-57	-59	41	5	-102	33
20	188	41	-35	-43	48	0	-31	3
30	121	38	-22	-20	41	-2	-5	2

Impedance Reduction

Unlike conventional IDs, the in-vacuum undulator is equipped with two special attachments to reduce the impedance in the electron path. One is an RF finger to smoothly connect the end of the magnet array and adjacent vacuum duct. The RF finger developed at SPring-8, called a flexible transition, is made of a woven strip of copper and can follow the movement of the ID gap from 8 mm to 50 mm (Figure 4). The other attachment is a thin metal foil covering the magnet surface. This is necessary because the magnet surface as seen by an electron is not smooth but has many gaps between adjacent magnet units.

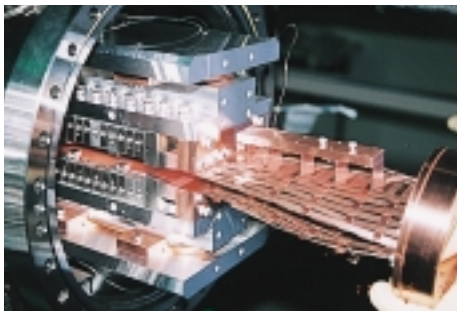

Figure 4: RF finger developed at SPring-8; the cooling water channel is attached before assembling all other components

In the first stage of in-vacuum undulator development, a 50 μm stainless steel sheet was used to cover the magnet surface and no cooling channel was attached to the RF fingers. In the beam test of this in-vacuum undulator at the ESRF in August 1996 [7], it was observed that the temperature of the RF finger rose 473 K and the beam was completely lost at a gap of 8 mm. In addition, the stainless steel was found to be partially melted after opening the vacuum chamber. To solve these problems, two improvements were made. One was to attach a cooling channel to the RF finger to remove the heat. The other was to replace the stainless-steel sheet with a 50 μm Ni sheet for thermal contact between the sheet and the magnet blocks by the attractive force. Because the magnet blocks are cooled by water during operation, heat originating in the sheet can easily escape. In addition, the Ni sheet is coated with a 10 μm copper layer to reduce the resistive wall heating.

Bake-out and Vacuum System

The bake-out system is one of the most important and difficult factors in constructing the in-vacuum undulator. Specifically, there are two important requirements. One is that the temperature of the magnet should not exceed 408 K to avoid demagnetization. The other is that the difference in heat expansion between the aluminum beam and the vacuum chamber (made of stainless steel) should be within 1 mm so that no unnecessary stress is placed on the RF fingers and bellows, these absorb the movement of the gap. To meet these requirements, the temperature of the magnet arrays is finely controlled with pressurized hot water to keep it at 403 K during the 48-hour bake-out process.

The in-vacuum undulator contains a large number of components. For example, the number of magnet blocks and holders is over two thousands. Accordingly, six ion pumps capable of 125 l/sec and twelve NEG pumps (non-evaporated getter pumps), capable of 500 l/sec are attached to obtain sufficient pumping speed. The surface of each magnet block is coated with a 5 μm layer of TiN to avoid outgas from pure-permanent magnet material.

After assembling all components of the first in-vacuum undulator except for the connecting parts between the device and the vacuum duct of the storage ring, an off-line vacuum test was performed. Figure 5 shows the results. The horizontal axis shows time after the end of the bake-out process and the vertical axis shows pressure. Two values of the pressure measured by different ion gauges attached to the upstream and downstream segments are shown. The figure shows that there is no difference between the upstream and downstream pressures and that a pressure is 5.6×10^{-9} Pa can be achieved, which is sufficient for installation in the storage ring.

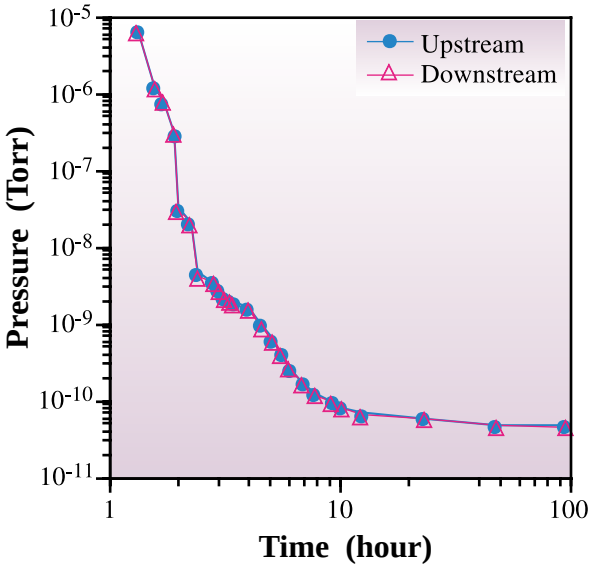

Figure 5: Off-line result of vacuum test of the in-vacuum undulator (pressure is shown as a function of time after the end of the bake-out process).

Installation and First Observation

The first four in-vacuum undulators were installed in the SPring-8 storage ring between November 1996 and February 1997. The pressure of all these devices reached below 1×10^{-8} Pa after the bake-out process. One of them was a vertical undulator having a horizontal magnetic field instead of a vertical field to obtain vertically polarized radiation [9]. After commissioning of the storage ring, the first radiation of the in-vacuum undulator installed at the beamline BL47XU was observed in April 1997. Figure 6 shows a photograph taken at that time. The radiation from the in-vacuum undulator irradiated a screen monitor located at the front-end section of the beamline. The gap was 20 mm and the storage-ring current was 0.047 mA. The bright circle seen in the center is the radiation from the in-vacuum undulator.

Figure 6: Photograph of screen monitor irradiated by radiation from the in-vacuum undulator.

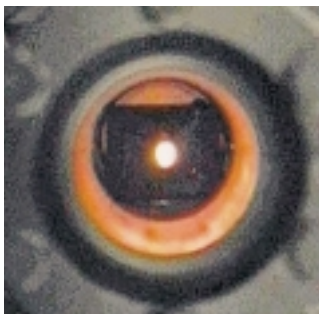

Operation

At present, twelve in-vacuum undulators are in operation at SPring-8. In the early operation, a degradation of lifetime was observed while closing the gap. For example, the lifetime degraded 30% at gap of 8 mm. Such degradation has not been observed recently due to improvement of the storage ring's vacuum. Thanks to the improvements described in Section 4, no significant temperature rise in RF finger and magnet arrays has been observed so far. The closed orbit distortion (COD) during tuning of the photon energy, *i.e.*, changing the ID gap, has been corrected by steering coils located upstream and downstream of the ID. After such COD correction, it was found that the displacement and the deflection due to tuning are within 10% of the electron-beam size and divergence, respectively. Measurements of radiation spectra from the in-vacuum undulators have been performed at various beamlines and have shown that the measured spectral shape is equivalent to our expectations.

Summary

Construction and operation of the in-vacuum undulator at SPring-8 have been described. Many other techniques besides those described here have been developed in construction and operation of the in-vacuum undulator. These all techniques have been applied to constructing not only in-vacuum undulators but also other IDs such as elliptic wiggler, helical undulator and figure-8 undulator.

References

[1] H. Kitamura, *J. Synchrotron Rad.* **5** (1998) 184.
[2] X. M. Marechal *et al., J. Synchrotron Rad.* **5** (1998) 431.
[3] T. Hara *et al., J. Synchrotron Rad.* **5** (1998) 403.
[4] T. Hara *et al., J. Synchrotron Rad.* **5** (1998) 426.
[5] T. Tanaka *et al., J. Synchrotron Rad.* **5** (1998) 459.
[6] R. P. Walker, *Nucl. Instrum. Meth. A* **335** (1993) 328.
[7] T. Tanaka *et al., SPring-8 Annual Report* (1998).
[8] S. Kirkpatrick *et al., Science* **220** (1983) 671.
[9] T. Tanaka *et al., J. Synchrotron Rad.* **5** (1998) 414.

Takashi Tanaka and Hideo Kitamura
SPring-8 / RIKEN·JASRI